Performance of Semi Active Lateral Control (SALC) Algorithm for Semi Active Suspension System in Multibody Co-Simulation Method

*M. M. Abdul Majid[*1], M. S. Salleh[1], M. A. Abu Hashim[1], N. H. Ismail[1], S. Mansor[2], S. A. Abu Bakar[2]*

[1]Department of Computer Aided Engineering (CAE), Vehicle Development and Engineering (VDE), Proton Holding Berhad, 40918 Shah Alam, Selangor

[2]Department of Aeronautics, Automotive and Ocean Engineering, Faculty of Mechanical Engineering, Universiti Teknologi Malaysia, 81310 Skudai

[*]marzukam@proton.com

ABSTRACT

The publication presents a controller strategy used in development of Semi Active Lateral Control (SALC) algorithm for passenger vehicle in enhancing transient handling performance using multibody co-simulation approach. Most of research in semi active suspension are focusing on ride comfort performance instead of handling due to nature of damping definition as energy dissipation element. Thus limiting benefits on handling characteristic with current available algorithms. The research scope covered experimental measurements, simulation model correlation, and vehicle plant modelling using multibody approach (MSC Adams/Car), controller algorithm development in Matlab/Simulink and performance validation in co-simulation environment. The test vehicle was instrumented with Racelogic's measurement tools for physical measurement on transient Step Steer manoeuvre. The experimental data used for simulation model correlation and validation. New controller algorithm (SALC) was than developed in Matlab/Simulink and integrate with correlated vehicle plant model for handling performance validation against passive suspension and Skyhook. The integration approach between MSC Adams/Car and Matlab/Simulink

ISSN 1823- 5514, eISSN 2550-164X

Received for review: 2017-07-31
Accepted for publication: 2018-03-30
Published: 2018-08-15

known as co-simulation or Software in the Loop (SiL), involve multiple solvers in one computational loop. In this research, the proposed SALC algorithm shows a significant improvement on transient handling (Step Steer), up to 21.8% in comparing to Skyhook performance. Thus led to the conclusion on additional benefits of semi active suspension system in handling performance beside ride comfort.

Keywords: *Semi Active Lateral Control (SALC), Semi Active Suspension System, Multibody Dynamics (MBD) and Multibody Co-Simulation Approach.*

Introduction

Limitation of passive suspension system in ride comfort and handling performance has led to considerable research in semi active suspension. Due to fixed value of damping rate in passive suspension system, vehicle response is varying according to the changes of vehicle setup e.g. weight and lateral acceleration (latacc) input. This circumstance creates undesired inconsistent response which led to uncomfortable driving feels across wider range of vehicle input. One of the critical characteristic measured in handling performance evaluation is roll overshoot and rise time (time to 90% steady state) in transient step steer test manoeuvre (ISO 7401:2011, Road vehicles - lateral transient response test method).

As specified in ISO 7401:2011 standard procedure for step input test, vehicle will be subjected to constant longitudinal velocity, 90km/h and several setting of steering wheel input will be given at 0.1s time step to reach desired range of lateral acceleration (0.1g, 0.3g and 0.5g). There is no feedback required from test driver for vehicle correction as the test classified as open loop manoeuvre. Responses from vehicle e.g. roll and yaw angle will be measured to quantified transient behaviour for further suspension tuning activities. Figure 1 shows an example of roll transient response due to step steer input test.

When vehicle undergo cornering event at constant longitudinal velocity, changes on steering wheel angle input will generate different lateral acceleration and responses. This situation causes variation of roll overshoot with respect to different lateral acceleration. Due to limitation of fixed damping rate in passive suspension system, driver will experience inconsistent vehicle response which led to reduction of handling sensation and insecurity feel. Furthermore, the rise time of vehicle to reach steady state condition will be also increased. The higher lateral acceleration experienced by passive suspension vehicle, the slower vehicle response (higher rise time) can be expected which translated into less agility.

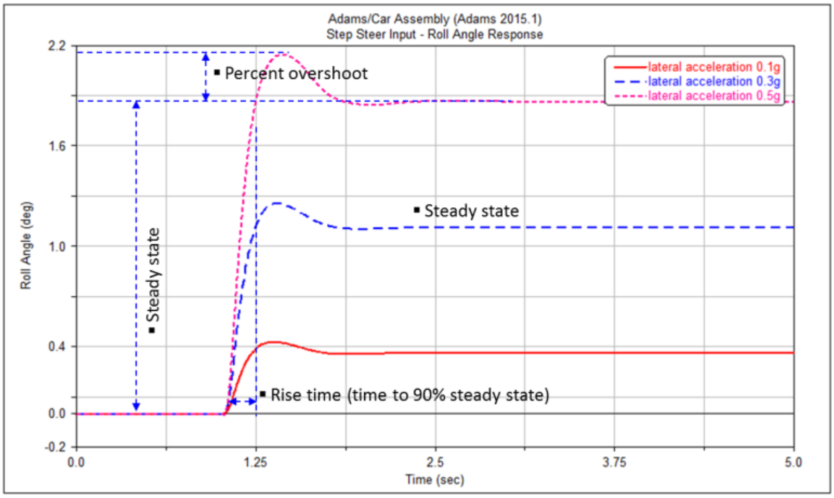

Figure 1: Vehicle response in transient step input [1].

Application of semi active suspension system allows wider range of force-velocity damping characteristic depending on controller strategy. However, most of research in semi active suspension system was focusing on ride comfort enhancement due to inability of controlling load transfer. In handling performance, load transfer is one of critical parameter determine vehicle traction ability especially on steady state handling performance. Due to the application of conventional spring rate in semi active suspension, there is no significant improvement on handling performance can be expected.

However, for transient handling performance, damping rate has a significant influence on roll overshoot and rise time. This paper explains the controller strategy used in integrating handling response parameter (lateral accelerator) into damping force calculation in comparing to conventional passive and Skyhook algorithm which solely rely on suspension velocity. The multibody approach used in modelling vehicle plant was also being introduced, to captured high fidelity simulation result.

Vehicle Plant Model using Multibody Approach

Multibody approach allows a complex modelling of suspension system and provides robust solution to solve motion problem. The multibody software such as MSC Adams/Car will formulate and solve the equations of motion for any boundary condition e.g. static, quasi-static, kinematic or dynamic. Rigid body and constraint properties are the basis formulation of motion equations, consist of expressions for kinetic and potential energy of multibody system. Adams/Solver use Euler-Lagrange equation for computational calculation.

The Lagrangian of dynamics system is a difference of kinetic energy (T) and potential energy (V), which written in the form of [2];

$$L = T - V \tag{1}$$

For multibody dynamics, the Lagrangian written by;

$$L = \sum_{j=i}^{N} T_j - V_j \tag{2}$$

Where $T_j - V_j$ are the kinetic energy and potential energy for each part (N) consist in the multibody system. The motion equation of multibody system is given by;

$$\frac{d}{dt}\left(\frac{\partial L}{\partial q}\right) - \frac{\partial L}{\partial q} + \Phi_q^T \lambda = Q \tag{3}$$

Where q is the column matrix of generalized coordinate, Φ_q is the $n \times m$ array which couples the constraints condition, n is the number of constraint's coordinate and m is number of constraints and λ is the column matrix of $n < m$ Lagrange multipliers. Adams/Solver use Newton method to solve Equation (3).

Modelling of vehicle simulation model was conducted in MSC Adams/Car. It is involved a parametric modelling of suspension geometry and state variables generation for compliance properties based on the measured components data from supplier. The frameworks of modelling full vehicle model in MSC Adams/Car started with template base preparation of vehicle sub-systems e.g. front suspension, rear suspension, steering system, tyre and body model.

Each sub-system was generated in Adams/Car Template Builder environment and integrate into assembly model in Adams/Car Standard Interface. Communication interface between those sub-systems were configured via input/output Communicators; defined in Template Builder environment. It is important to ensure those Communicators match between action and reaction parts to avoid unnecessary grounded which led to error in analysis convergence. Figure 2 shows the full vehicle assembly of simulation plant model in MSC Adams/Car.

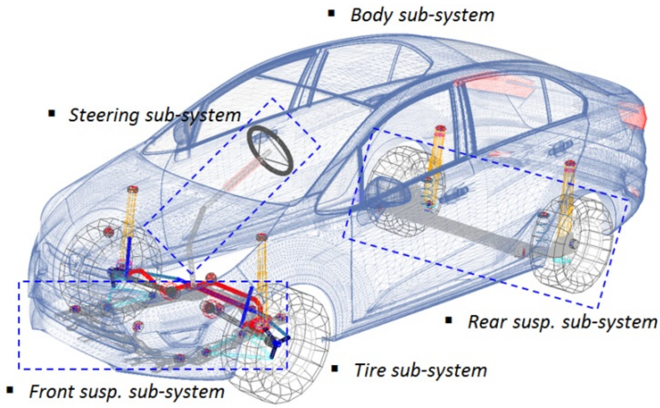

Figure 2: Assembly of vehicle simulation model in MSC Adams/Car.

Front suspension model

The parametric modelling of front suspension geometrical model was based on hardpoints position as Figure 3. Assumption values e.g. mass, CoG position and mass moment of inertia were considered for each components. Those values to be tuned in later stage of simulation model correlation.

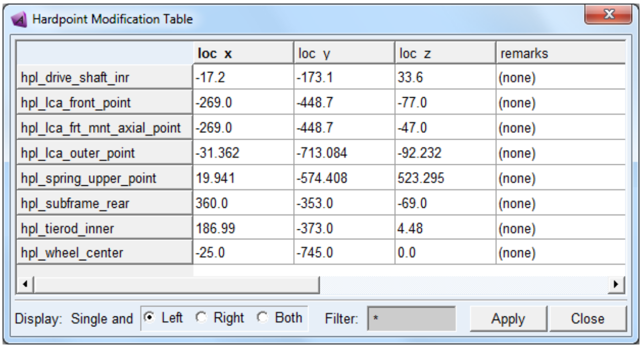

Hardpoint Modification Table

	loc x	loc y	loc z	remarks
hpl_drive_shaft_inr	-17.2	-173.1	33.6	(none)
hpl_lca_front_point	-269.0	-448.7	-77.0	(none)
hpl_lca_frt_mnt_axial_point	-269.0	-448.7	-47.0	(none)
hpl_lca_outer_point	-31.362	-713.084	-92.232	(none)
hpl_spring_upper_point	19.941	-574.408	523.295	(none)
hpl_subframe_rear	360.0	-353.0	-69.0	(none)
hpl_tierod_inner	186.99	-373.0	4.48	(none)
hpl_wheel_center	-25.0	-745.0	0.0	(none)

Display: Single and Left Right Both Filter: * Apply Close

Figure 3: Hardpoints parameters for front suspension model.

The front suspension system (Figure 4) consists of subframe, knuckle, lower control arm (LCA) and strut assembly (absorber and top mount). Those components were connected with compliance joints e.g. bush elements, damper and spring force. For high fidelity simulation result, a flexible body of subrame was used to capture structure stiffness and dynamics mode shape. It is important since the analysis workscope involve vehicle response measurement e.g. roll and steering wheel angle at high lateral acceleration test (up to 0.7g lateral acceleration range).

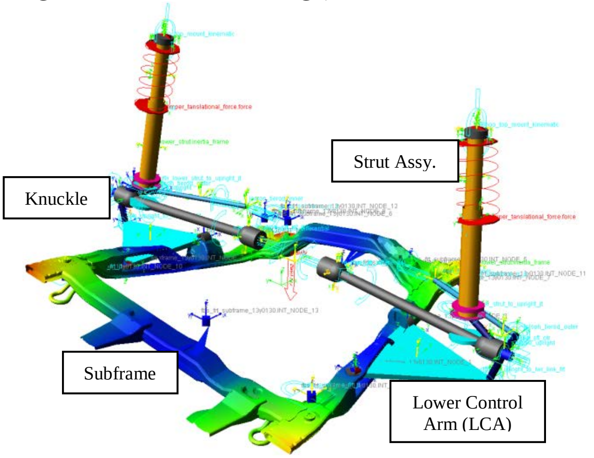

Figure 4: Front suspension model (McPherson Strut).

Stiffness and damping data on each bush properties used in the simulation model were based on actual measurement data from component supplier. Only static stiffness value (Ks) was captured the simulation model. The modelling of bush element between two components (action, I-part and reaction, J-part) is governed in Equation (4) where $[k_i]$ is matrix of bush stiffness for each directions, $[x_{i12}]$ is displacement of marker I and marker J, $[c_i]$ is matrix of bush damping rate and $[v_{i12}]$ is velocity of marker I and marker J. For non-linear bush stiffness, AKIMA spline syntax was applied in MSC Adams/Car as Equation (5).

$$[F_i] = [[k_i].[x_{i12}]] + [[c_i].[v_{i12}]] \tag{4}$$

Where, MSC Adams syntax for non-linear bush model is:

$$\begin{aligned}[F_i] = akispl.(D_i(MARKER\_I, MARKER\_J, MARKER\_J), 0, [k_i]) \cdots \\ + ([c_i].V_i(MARKER\_I, MARKER\_J, MARKER\_J)\end{aligned} \tag{5}$$

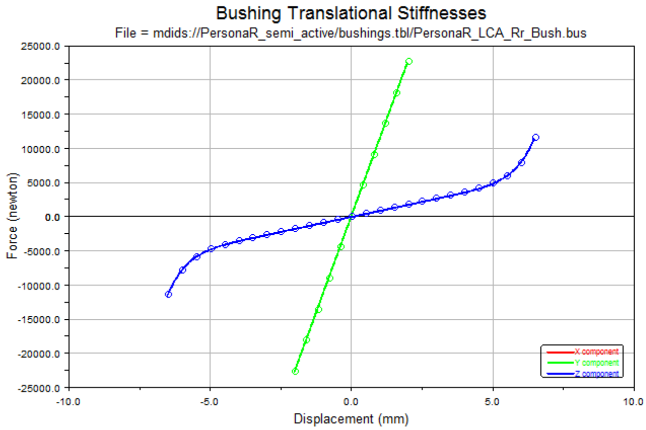

Figure 5: Bush stiffness properties of rear LCA mount.

Rear suspension model

The critical modelling of rear suspension model is flexible body of torsion beam. Roll stiffness, kinematic roll center height (KRCH), toe and camber change characteristic were rely on stiffness matrix and geometrical of rear axle's modal neutral file (.mnf). The remaining elements e.g. bush, spring and damper force were modelled using similar method in front suspension.

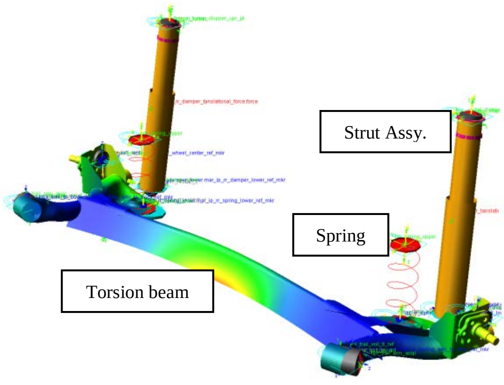

Figure 6: Rear suspension model (torsion beam).

Steering system

Steering system is one of the important sub-systems in this analysis workscope. Step steer analysis rely on steering characteristic; where vehicle responses e.g. roll and yaw rate depending on steering wheel angle. Although the actual model used Electronic Power Steering (EPS) system which programmed to have multiple steering assist curve, a simplified modelling of steering assistance was used due to non-related steering effort analysis. The steering sub-system is connected to front suspension model via interface communicator.

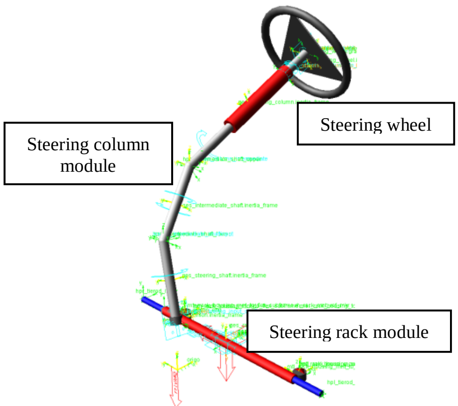

Figure 7: Steering sub-system model.

A dummy steering assist curve (Figure 8) was used in the form of MSC Adams syntax as governed in Equation (6). This formulation applied into force element as represented in Figure 9; acting in parallel directional to steering rack.

$$F_{steer} = piston\_area\,.[AKISPL(AZ(MARKER\_I, MARKER\_J).RTOD), \ldots \\ \ldots 0, steering\_assist\_curve] \quad (6)$$

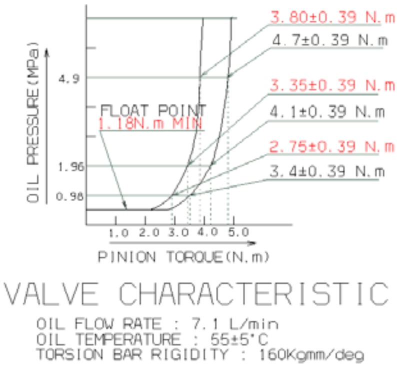

Figure 8: Dummy steering assist curve [3].

The most important steering property for this research work scope is rack ratio. This model used rack ratio, 50.8mm/rev and rack stroke, ±74.9mm which translated into maximum 2.94rev (steering wheel lock to lock turn). The rack ratio value is represented with reduction gear element in MSC Adams/Car as Figure 10.

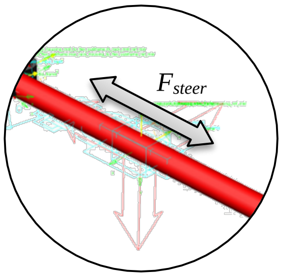

Figure 9: Steering assist force

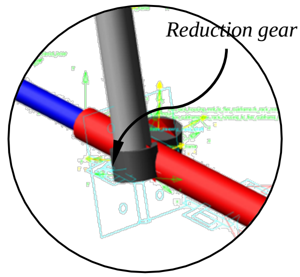

Figure 10: Reduction gear element

Controller Integration Using Co-simulation Approach

There are several methods in integrating controller algorithm with vehicle plant model. Most common approach is via linearized or simplified mathematical model in Matlab Simulink [4]. However, multibody approach offers higher fidelity model with more vehicle parameters to be captured.

In co-simulation approach, two different solvers will be used concurrently in solving multibody problem. In this paper, the solvers involved are Adams/Solver for motion equation problem and Matlab/Simulink for damping force calculation. Those solvers communicated through input/output plant signals which have to be defined in both environments.

There are total thirteen state variables created in this vehicle simulation model; four plant input signals of damping force and nine plant output signals for sprung velocity, unsprung velocity and vehicle lateral acceleration (Figure 11). The plant output signals will be passed to Matlab/Simulink and the calculated plant input signals will be send back to MSC Adams/Car. Those communication will be continuously interact as a one loop of co-simulation analysis which also known as Software in the Loop (SiL).

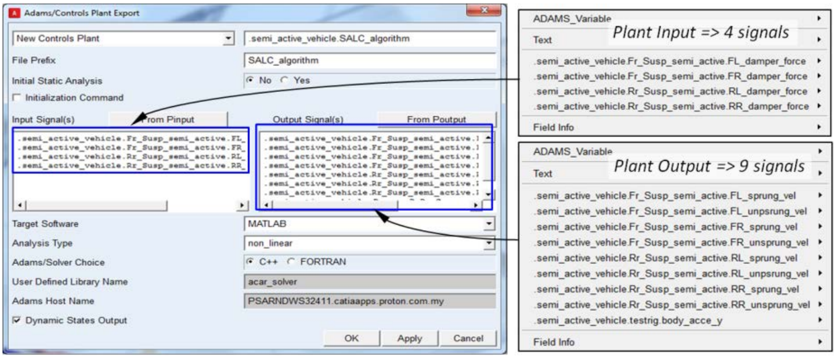

Figure 11: Plant input/output configuration in MSC Adams/Car.

Plant input/output signals are the representation of state variable use in motion equation e.g. damper force, unsprung velocity etc. It is a series of general equation written in the form MSC Adams syntax. The basic formulation of passive damping is governed by Equation (7). However, for semi active suspension model, the damping force will be calculated by controller algorithm in Mathlab/Simulink.

$$F_d = C \times v_{12} \tag{7}$$

Where v_{12} is suspension relative velocity and C is damping rate either in constant value or algorithm form. The measurement of v_{12} in MSC Adams/Car is represented by run-time state variable written in Adams syntax for format as;

$$VZ(.dal\_j\_1,\ .dal\_i\_1,\ .jxl\_j\_10) \tag{8}$$

Where VZ is a MSC Adams expression to measure velocity in z-axis direction, $.dal\_j\_1$ is marker of second vector point, $.dal\_i\_1$ is marker of first vector point and $.jxl\_j\_10$ is reference marker orientation. Adams syntax in Equation (8) was used for the remaining suspension relative velocity measurement (sprung and unsprung velocity) for each suspension corners with specific marker attachments.

The direction of damping force and suspension velocity measurements was defined according to strut orientation. Figure 12 shows state variable definition for damping force in MSC Adams/Car which to be calculated by Matlab/Simulink co-simulation.

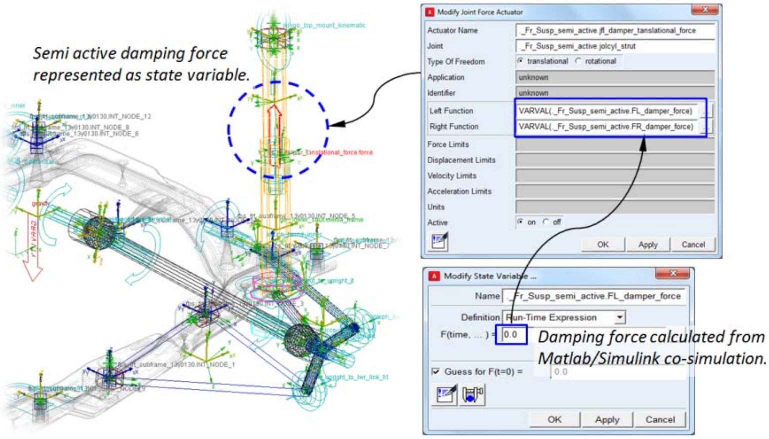

Figure 12: Semi Active damping force modelling.

Adams block in Matlab/Simulink (Figure 13) was then configured with information of Adams/Solver setting e.g. location Adams Command File (.acf), communication interval time and integrator setting. Execution of analysis was done in Matlab/Simulink environment which then activate both parallel solvers.

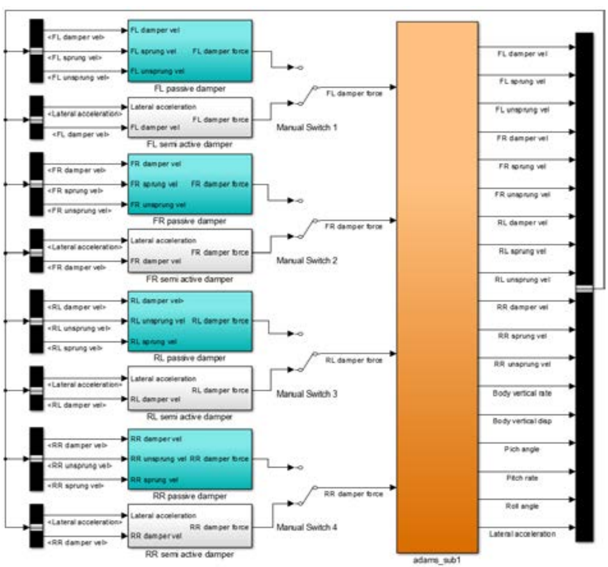

Figure 13: Integration of MSC Adams in Matlab/Simulink environment.

Experimental Measurement & Model Validation

For the purpose of simulation model validation, there are two experimental measurements were conducted on passive suspension vehicle model. Results from actual measurement were then used for simulation model updating and validation.

The first experimental measurement is vehicle static, Center of Gravity (CoG) and vehicle corner weight. It was conducted based on two setup; normal position for longitudinal CoG and tilt position for vertical CoG (Mango, N., 2004). The measurement was conducted using Intercomp SW650RFX™ where the test vehicle was placed on each portable weight pads. In normal vehicle position, both front and rear axle weight (W_r and W_f) were measured for longitudinal CoG calculation. Axle weight is defined as submission of each vehicle corner weight. A simple free-body diagram calculation (Figure 14) was then conducted for vehicle CoG (x and y-axis) definition as governed in Equation (9).

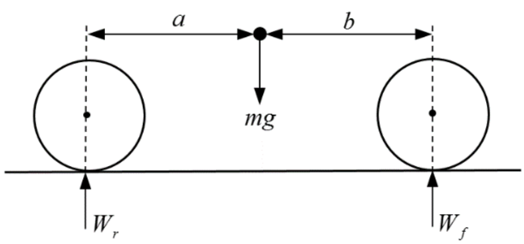

Figure 14: Free-body diagram of normal vehicle position measurement.

For x-axis and y-axis vehicle CoG calculation, only plane z-x plane was considered. The submission of moment at front tyre center point, $\sum M_{W_f}$ can be written in Equation (9);

$$W_r.(a+b) - mg.(a) = 0 \tag{9}$$

Where W_r is the measurement of rear axle weight (average value), $(a+b)$ is wheelbase size and a is vehicle CoG in x-axis. The same formulation used for vehicle CoG in y-axis.

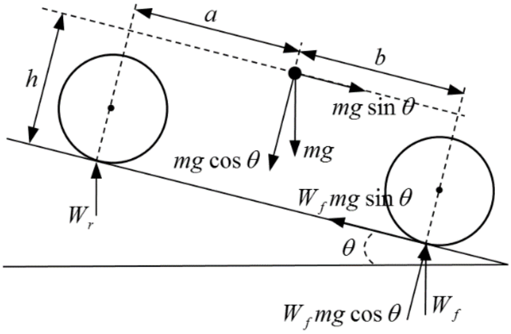

Figure 15: Free-body diagram of tilt vehicle position measurement.

For CoG z-axis measurement, vehicle was tilted as free-body diagram in Figure 15 and vehicle axle weight of front and rear were recorded. The calculation of vehicle CoG z-axis was based on submission moment at rear tyre contact patch as governed in Equation (10).

$$mg.\cos\theta.b + mg.\sin\theta.h - W_f.\cos\theta.(a+b) = 0 \qquad (10)$$

Where W_f is the measurement of front axle weight (average value), $(a+b)$ is wheelbase size, b is x-axis distance of vehicle CoG to rear wheel center, is h vehicle CoG in z-axis and θ is angle of vehicle being tilted. The static measurement data of vehicle CoG and corner weights were then being updated into base simulation model.

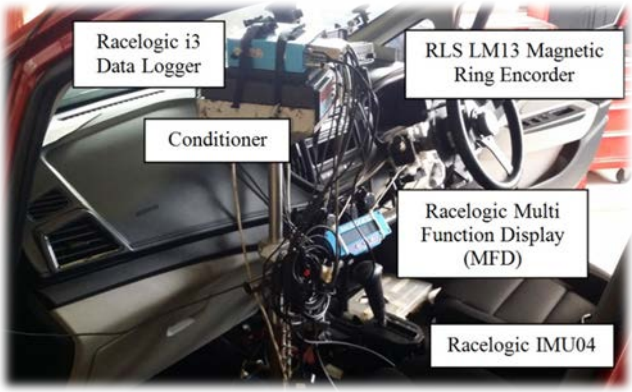

Figure 16: VBOX Racelogic instrumentation for Step Steer measurement.

The second experimental test conducted was transient step steer input manoeuvre. Main instrumentations used were Inertial Measurement Unit (VBOX Racelogic IMU04) and steering angle sensor (RLS LM13 magnetic ring encoder) which connected to VBOX Racelogic 3i Data Logger (Figure 16). The test was conducted at mid laden condition (with driver and front passenger weight) at constant speed 90km/h with various steering wheel angle input to meet 0.3g, 0.5g and 0.7g lateral acceleration as per required in test requirement. Measurement data shows good correlation with simulation result.

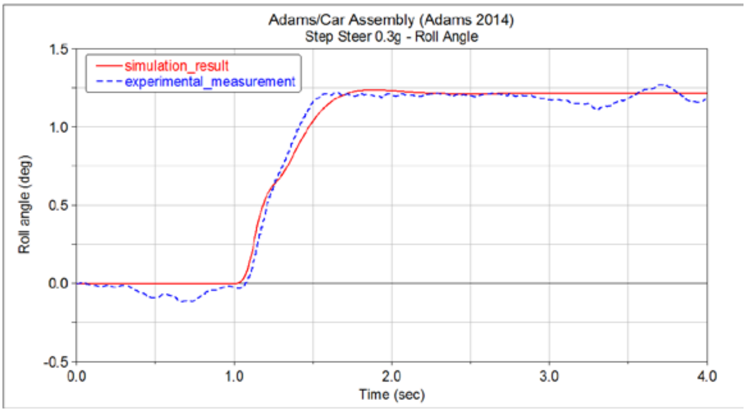

Figure 17: Transient roll angle at 0.3g lateral acceleration.

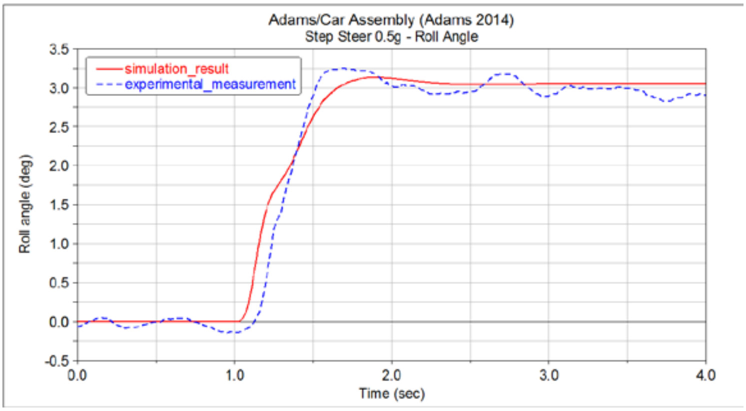

Figure 18: Transient roll angle at 0.5g lateral acceleration.

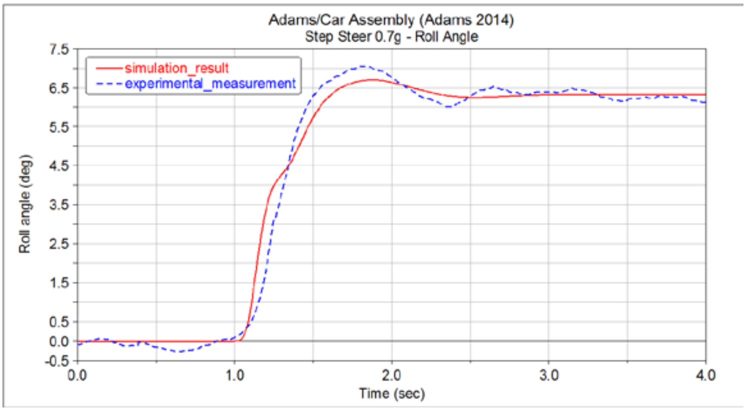

Figure 19: Transient roll angle at 0.7g lateral acceleration.

Semi Active Lateral Control (SALC) Algorithm Strategy

In comparing the performance of new Semi Active Lateral Control (SALC) algorithm, Skyhook algorithm was also modelled and integrated into vehicle simulation model. The Skyhook algorithm was introduced by Karnopp [5], with the objective is to control sprung mass motion. An imaginary damper was introduced in between sprung mass and stationary sky with intention to provide more damping force to sprung mass.

Control strategy of Skyhook algorithm can be summarized as; if product of sprung mass velocity, v_1 and relative velocity between sprung and unsprung mass, v_{12} is positive, then semi active damping force is proportional to velocity of sprung mass. Else, the semi-active damping force will be set as zero. Skyhook algorithm can be written as Equation (11);

$$\begin{array}{llll} If & v_1.v_{12} \geq 0 & then & F_d = C_{sky}.v_1 \\ If & v_1.v_{12} < 0 & then & F_d = 0 \end{array} \tag{11}$$

Where v_1 is sprung mass velocity, v_{12} is suspension relative velocity, C_{sky} is Skyhook damping rate and F_d is Skyhook damping force.

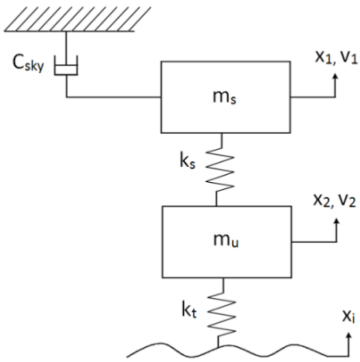

Figure 20: Ideal Skyhook control system.

Since the Skyhook control policy is to provide more damping on sprung mass, Skyhook damping force will be only applied when relative velocity of sprung mass to unsprung mass (v_{12}) is positive (i.e. when v_1 is greater than v_2 or if the direction of v_1 in downward direction). When sprung mass move downward with negative velocity ($-v_1$), the Skyhook damping force should be applied in positive direction ($+x_1$). However, in semi-active damper configuration, it is still in tension which in negative direction ($-x_1$).

Since semi-active damping force cannot possibly be applied in similar direction as Skyhook damping force, the best solution is to minimize the damping force. Ideally, the semi-active damper for case $v_1.v_{12} < 0$ is desired to be no damping force, but in reality there is some small damping force present. Although the direction is not similar to Skyhook damping force but the smaller magnitude of damping force can be considered negligible.

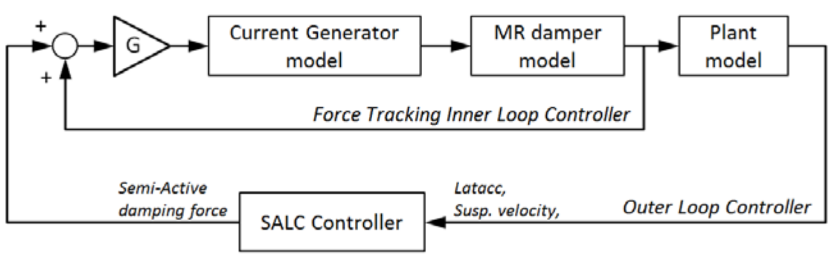

Figure 21: Layout of semi-active SALC controller model.

Figure 21 shows Semi Active Lateral Control (SALC) controller layout for Magnetorheological (MR) damper semi active suspension application. In order to optimize transient handling performance, SALC algorithm applied vehicle lateral acceleration signal as conditional setting. The concept of integrating lateral acceleration input in semi active suspension algorithm was initiated by Takayoshi [6], through his gain schedule H∞ controller. An additional damping force will be added on top of conventional damping force-velocity base; in providing more energy dissipation at higher lateral acceleration condition. As a result, vehicle handling response at lower and higher lateral acceleration can be retained closer thus improving transient handling limitation as stated in the introduction chapter. The SALC algorithm is governed by;

$$\begin{array}{llll} If & 0g \le latacc \le 0.3g & then & F_d = C_{low}.v_{12} \\ If & 0.31g \le latacc \le 0.5g & then & F_d = C_{med}.v_{12} \\ If & latacc \ge 0.7g & then & F_d = C_{high}.v_{12} \end{array} \qquad (12)$$

Where v_{12} is suspension relative velocity, C_{low} is SALC low damping rate, C_{med} is SALC medium damping rate, C_{high} is SALC high damping rate and F_d is SALC damping force.

Result and Discussion

The performance comparison of SALC algorithm was done based on transient Step Steer analysis. There are three parameters have been validated; peak roll, roll overshoot and rise time. Both SALC and Skyhook algorithm were tuned to meet closer to passive suspension performance at 0.3g lateral acceleration. Table 1 shows almost similar performance between SALC and passive suspension. However more roll overshoot observed on Skyhook which based on the optimized setting between lower and higher lateral acceleration performance.

Table 1: Improvement on roll transient at 0.3g lateral acceleration

Responses	**Passive**	**Skyhook**	**Imprv. (%)**	**SALC**	**Imprv. (%)**
Peak roll (deg)	1.24	1.26	-1.6	1.24	0.0
Roll overshoot (deg)	0.02	0.04	-100.0	0.02	0.0
Rise time (s)	1.55	1.56	-0.6	1.55	0.0
Average Performance			-34.1		0.0

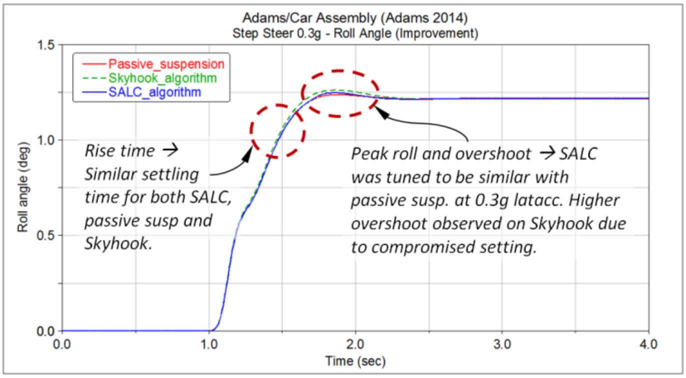

Figure 22: Improvement on roll transient → 0.3g lateral acceleration.

Better improvement observed on SALC at 0.5g lateral acceleration due to higher damping force with average of 13.4% improvement. Roll overshoot for SALC was closer to the value at 0.3g lateral acceleration which translated into better roll overshoot difference. It is also observed that better rise time on SALC due to minimum overshoot. Figure 22 shows minimal roll overshoot for SALC in comparing to passive suspension and Skyhook. However, no changes observed on steady state value due to no influence by damper rate.

Table 2: Improvement on roll transient at 0.5g lateral acceleration

Responses	**Passive**	**Skyhook**	**Imprv. (%)**	**SALC**	**Imprv. (%)**
Peak roll (deg)	3.14	3.18	-1.3	3.10	1.3
Roll overshoot (deg)	0.08	0.12	-50.0	0.05	37.5
Rise time (s)	1.58	1.60	-1.3	1.56	1.3
Average Performance			-17.5		13.4

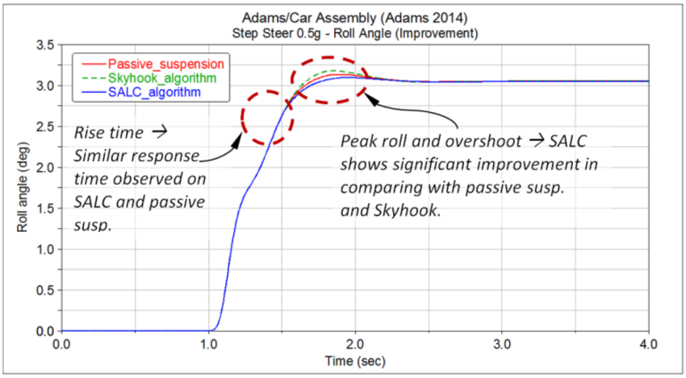

Figure 23: Improvement on roll transient → 0.5g lateral acceleration.

As for the higher lateral acceleration input, the handling performance improvement on SALC is more prominent. The average of 24.2% improvement observed in comparing to passive suspension system. Roll overshoot for SALC is closer to 0.5g and 0.3g lateral acceleration condition although with slight increment observed. The rise time is generally faster than both Skyhook and passive suspension due to smaller overshoot. As per expected, SALC algorithm shows a significant improvement on transient handling performance especially at higher lateral acceleration input.

Table 3: Improvement on roll transient at 0.7g lateral acceleration

Responses	**Passive**	**Skyhook**	**Imprv. (%)**	**SALC**	**Imprv. (%)**
Peak roll (deg)	6.71	6.63	1.2	6.49	3.3
Roll overshoot (deg)	0.38	0.36	5.3	0.13	65.8
Rise time (s)	1.65	1.63	1.2	1.58	4.2
Average Performance			2.6		24.4

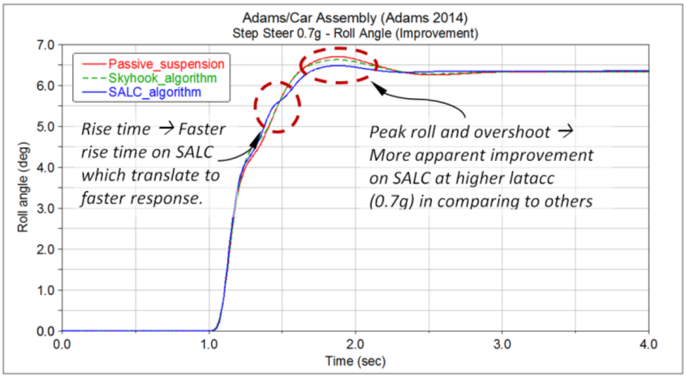

Figure 24: Improvement on roll transient → 0.7g lateral acceleration.

Figure 25 shows clearer illustration on overall SALC algorithm improvement for transient handling characteristic. With SALC application, consistent peak roll and overshoot can be achieved across different lateral acceleration input which translated into better handling performance as per discussed in introduction chapter. In comparing to conventional passive suspension system, more overshoot and higher peak roll are expected due to constant damping rate. In fact, the SALC shows better transient handling performance compared to Skyhook algorithm due to additional damping force introduction at higher lateral acceleration condition.

In addition, faster rise time observed on SALC performance especially at higher lateral acceleration input (0.7g) compared to conventional passive suspension which getting towards slower rise time. With the improvement of faster rise time on SALC, overall vehicle handling performance is expected to be more responsive and agile at any range of lateral acceleration input.

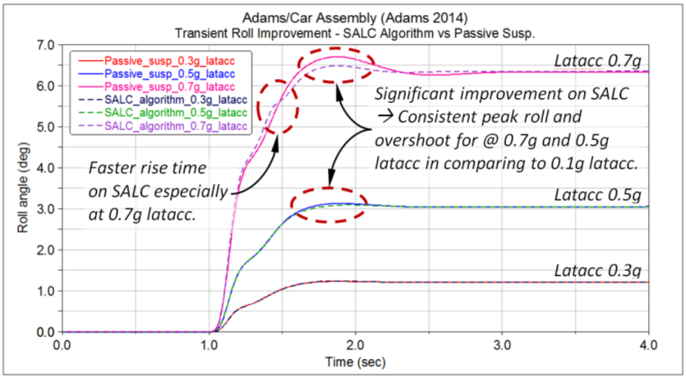

Figure 25: Overall SALC performance - transient handling improvement.

Conclusion

Semi active suspension system is well known to be better performance in comparing to passive suspension. With wider range of damping rate, it is allow wider spectrum of suspension tuning with regards to ride comfort. Since damper is known as energy dissipation element, less significant improvement expected on handling performance with the application of semi active suspension system. However with SALC algorithm, significant improvement observed on transient handling performance with minimal roll overshoot across wider range of lateral acceleration input. Furthermore, faster vehicle response and agility is expected with the application of SALC algorithm which translated based on faster rise time at any range of lateral acceleration input. In this paper, it is confirmed that SALC algorithm is able to minimized roll overshoot different between various lateral acceleration input for better handling performance.

Acknowledgement

The authors wish to thank you to Perusahaan Otomobil Nasional Sdn. Bhd. (Proton) and Universiti Teknologi Malaysia (UTM) in providing the opportunity and support in publishing this research topic.

References

[1] K. . Kasmijan, "P2-30A Vehicle Handling Performance," (2012).
[2] J. McConville, J. and McGrath, "Introduction to ADAMS Theory," (1998).
[3] Abdul Majid, M. M., "P2-30A ISO Lane Change Analysis Performance," (2012).
[4] S. A. Abu Bakar, "Modelling and Control of Magnetorheological Damper in Semi-Active Suspension System of Passenger Vehicle," (2009).
[5] D. Karnopp, M. J. Crosby, and R. A. Harwood, "Vibration Control Using Semi - Active Force Generators," *ASMEJournal Eng. Ind.*, vol. 96 (2):619, (1974).
[6] T. Fujita, T. Fukao, T. Kinoshita, and N. Itagaki, *Semi-active suspension improving both ride comfort and handling feel*. IFAC, (2013).